



## DISPLACEMENT BASED FLEXURE-SHEAR CAPACITY MODELS FOR BRIDGE COLUMNS UNDER SEISMIC LOAD

J.-H. Lee<sup>1</sup>, S.-H. Ko<sup>2</sup>, J.-H. Choi<sup>2</sup> and Y. S. Chung<sup>3</sup>

### ABSTRACT

Reinforced concrete columns with relatively small aspect ratios show flexure-shear behavior, which is flexural behavior at initial and medium displacement stages and shear failure at final stage. These type of columns have lower ductility than those with flexural failure. Therefore, displacement based flexure-shear capacity models shall be applied as well as flexural capacity curves, in order to determine ultimate displacement for seismic design or performance evaluation. However, most current design codes for structural concrete describe shear strength equations that provide strength only without considering ductility capacity. Even for shear related action, however, the displacement-based design concept might be more appropriate, especially for seismic design. CALTRANS Seismic Design Criteria adopts the displacement based flexure-shear capacity model for reinforced concrete bridge column design and some researchers proposed displacement based flexure-shear capacity models. In order to investigate the displacement based flexure-shear capacity models, four full scale (diameter of 1.2 m) circular reinforced concrete columns were tested under cyclic lateral load with constant axial load. The main test variables are aspect ratio (1.825, 2.5, 4.0) and longitudinal steel ratio. Two more full scale (diameter of 1.2 m) circular reinforced concrete columns test results conducted by other researchers are also selected to compare with the models. The predicted failure mode by each model and accuracy are presented and discussed.

### Introduction

It is known that, reinforced concrete columns with shear span-to-depth ratios (aspect ratio in cantilever columns) between 1.5 and 3.0, show flexure-shear behavior. Those columns show flexure behavior at initial stage of seismic loading but fail by shear action at the final stage. This type of brittle failure was reported by many destructive seismic events, such as the Northridge earthquake in 1994 and the Kobe earthquake in 1995. These columns have lower ductility than those with flexural failure. Therefore, displacement based flexure-shear capacity models shall be applied as well as flexural capacity curve in order to determine ultimate displacement for seismic design or performance evaluation. However, most current design codes for structural concrete, except CALTRANS Seismic Design Criteria (2006), describe shear strength equations that provide strength only without considering ductility capacity. Even for shear related action, however, displacement-based design concept might be more appropriate especially for

---

<sup>1</sup>Professor, Dept. of Civil Engineering, University of Yeungnam, Gyoengsan city, Korea.

<sup>2</sup>PhD Student, Dept. of Civil Engineering, University Yeungnam, Gyoengsan city, Korea.

<sup>3</sup>Professor, Dept. of Civil Engineering, Chung-Ang University, Ansong city, Korea.

seismic design. The displacement based flexure-shear capacity models are quite useful to predict ultimate displacement of the columns with flexure-shear behavior. In addition, column failure mode can be predicted by these models with flexural capacity curve (lateral load-displacement curve) determined by push-over analysis.

The main objective of this research is to investigate the accuracy of each displacement based flexure-shear capacity model. For this purpose, full scale (diameter of 1.2 m) column tests were conducted to exclude size effects on the shear behavior. Four full scale circular reinforced concrete columns were tested under cyclic lateral load with constant axial load. The main test variables were aspect ratio (1.825, 2.5, 4.0) and longitudinal steel ratio. Two more full scale (diameter of 1.2 m) circular reinforced concrete column test results conducted by other researchers are also selected to compare with the models. The predicted failure mode by each model and accuracy are presented and discussed.

## Experiment

### Specimens and Test

Four large size circular reinforced concrete columns were constructed. All the columns have 1200 mm diameter cross-section and main variables are longitudinal steel ratio and aspect ratio (span-depth ratio). Total height of MS-HT4-N-L2 and MD-HT6-N-L2 specimen is 5920 mm and loading height is 4800 mm, so that the aspect ratio should be 4.0. Total height of MS-HT4-N-FS specimen is 4120 mm and loading height is 3000 mm, so that the aspect ratio should be 2.5. Total height of MS-HT4-N-SH specimen is 3310 mm and loading height is 2190 mm, so that the aspect ratio should be 1.825.

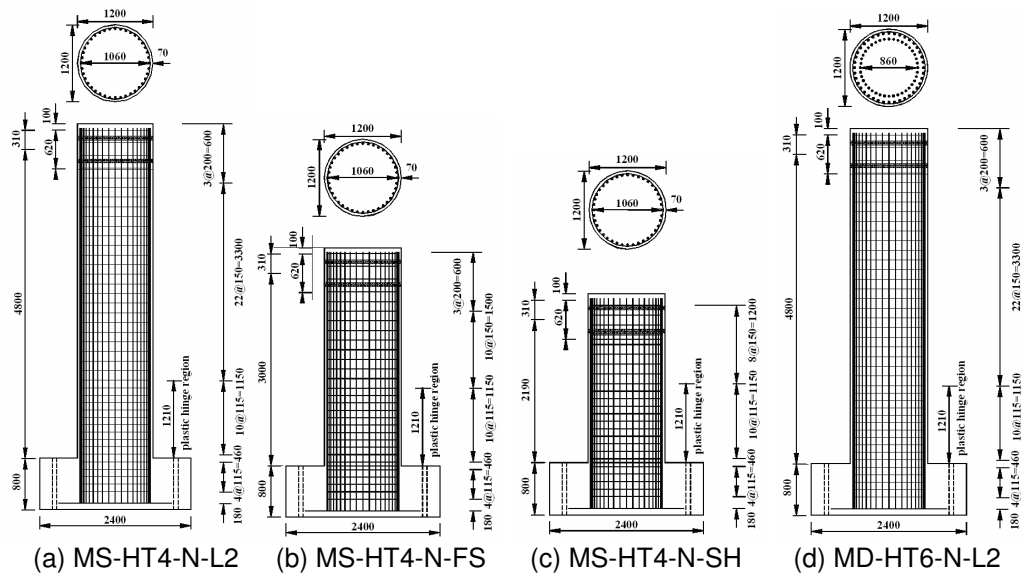


Figure 1. Configurations and dimensions of specimens.

D19 (diameter of 19 mm) and D10 bars were used as longitudinal reinforcement and transverse reinforcement, respectively, for all the column specimens. Details and variables of the column specimens are shown in Fig. 1 and Table 1. For the longitudinal reinforcement, 40-D19 and 80-D19 were used for MS-HT4-N series columns and MS-HT6-N-L2 column specimen, respectively, so that the steel ratio should be 0.0102 and 0.0203, respectively. D10 circular ties were provided as transverse reinforcement. In addition to the circular ties, crossties were used for MS-HT4 series columns as shown in Fig. 2. Perfect hoops by use of couplers were used for MD-HT60N-L2 column. Space of transverse steel in plastic hinge region was 115 mm for all the specimens, which resulted in volumetric ratio of 0.0023. It corresponds to 24% of the required confining steel ratio defined by AASHTO Specifications (2002) and Korean Bridge

Design Specifications (2005). Space of 115 mm in plastic hinge is equivalent to 6 times the longitudinal bar diameter and 12 times the transverse bar diameter.

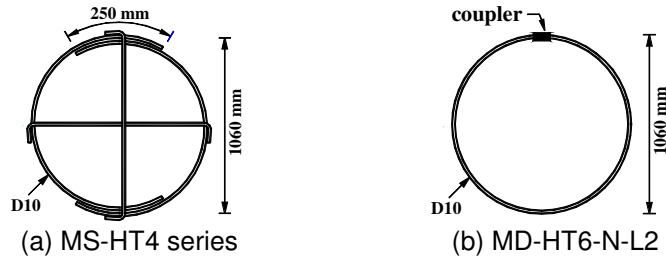


Figure 2. Configuration of transverse steel.

Material test was carried out to determine the actual mechanical properties of concrete and steel. The concrete compressive strength by 100 X 200 mm cylinder was 24.8 MPa at the time of loading test. Yield strength of the reinforcement was measured to be 343 MPa for D19 reinforcement and 373 MPa for D10 reinforcement.

Table 1. Test column details and material properties.

Specimens	Loading height (mm)	Aspect ratio	Longitudinal steel ratio	Transverse hoop tie			
				Plastic hinge region		Outside plastic hinge region	
				Volumetric ratio (%)	Space (mm)	Volumetric ratio (%)	Space (mm)
MS-HT4-N-L2	4,800	4.0	0.0102	0.23	115	0.175	150
MS-HT4-N-FS	3,000	2.5	0.0102				
MS-HT4-N-SH	2,190	1.825	0.0102				
MD-HT6-N-L2	4,800	4.0	0.0203				



Figure 3. Test setup.

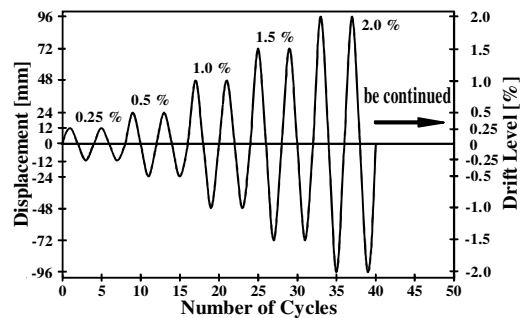


Figure 4. Loading pattern.

As shown in Fig. 3, quasi-static test was conducted under constant axial load and incrementally increasing lateral deformation reversals using Hydraulic actuator with  $\pm 500$  mm displacement capacity and 3500 kN force capacity. Axial load of 1863 kN was applied so that the axial load ratio should be 0.07. Two cycles of lateral load were applied at each drift level as shown in Fig. 4.

## Test Results

MS-HT4-N-L2 specimen (aspect ratio = 4.0) showed typical flexure failure in plastic hinge region, while the other three columns showed flexure-shear failure. Fig. 5 presents failure of MS-HT4-N-SH specimen (aspect ratio = 1.825), which shows diagonal cracks due to flexure and shear action. Fig. 6 shows failure of MD-HT6-N-L2 specimen. It shows flexure-shear failure even though its aspect ratio is 4.0. It is believed that relatively small amount of transverse steel compared with longitudinal steel resulted in diagonal cracks and shear related failure after plastic hinge formed by flexure at the bottom of column. Failure mode was eventually flexure-shear failure by fracture of transverse steel and shear cracks. It should be noted that MD-HT6-N-L2 specimen has twice the longitudinal steel ratio compared with MS-HT4-N-L2 specimen.



Figure 5. Failure of MS-HT4-N-SH.



Figure 6. Failure of MD-HT6-N-L2.

During the load test, lateral load and lateral displacement were measured up to failure. Envelop curves of the column specimens were obtained from the measured cyclic relationships, which will be compared with the displacement based flexure-shear capacity models. More information about the test can be found elsewhere (Chung et al. 2001).

### Displacement Based Flexure-Shear Capacity Models

#### CALTRANS

CALTRANS Seismic Design Criteria (2006) defines shear capacity model as Eq. (1) through (8) in SI units. The nominal shear strength is calculated as summation of contributions of concrete,  $V_c$ , and transverse reinforcement,  $V_s$ . CALTRANS defines shear strength of concrete,  $V_c$  differently by classifying inside the plastic hinge region and the rest. In  $V_c$  determination for the plastic hinge region, displacement ductility factor  $\mu_d$  is used as a main variable. The volumetric ratio of transverse steel, yield strength of transverse steel, and axial load effect are also considered in  $V_c$ . The shear effective area,  $A_e$  in Eq. (2), is taken as 0.8 times gross sectional area for circular sections. The shear strength of transverse steel,  $V_s$ , is calculated by Eq. (8) for circular sections based on 45° angle truss model, where  $A_{sp}$  is the area of hoop or spiral and  $D_{sp}$  is the diameter of core concrete measured between center to center of hoop or spiral.

$$V_n = V_c + V_s \quad (1)$$

$$V_c = v_c A_e \quad (2)$$

$$v_c = \text{Factor1} \times \text{Factor2} \times \sqrt{f'_c} \leq 0.33\sqrt{f'_c} \quad (3)$$

$$\text{Factor1} = \frac{\rho_s f_{yh}}{12.5} + 0.305 - 0.083\mu_d \quad (4)$$

$$0.025 \leq \text{Factor1} \leq 0.25 \quad (5)$$

$$Factor2 = 1 + \frac{P}{13.8A_g} \quad (6)$$

$$1.0 \leq Factor2 \leq 1.5 \quad (7)$$

$$V_s = \frac{\pi A_{sp} f_{yh} D_{sp}}{2s} \quad (8)$$

### Aschheim and Moehle

Aschheim and Moehle (1992) proposed Eq. (9) through (12) in SI units to compute the nominal shear strength of reinforced concrete columns. Considering displacement ductility and the effect of compression,  $V_c$  is calculated by Eq. (10) and (11) for plastic hinge region. The effective shear area,  $A_e$  in Eq. (10), is 0.8 times gross section area ( $0.8A_g$ ) for circular sections. The shear strength of reinforcement,  $V_s$ , is calculated by Eq. (12) based on  $30^\circ$  angle truss model, and  $0.8D$  is used for  $d$  in circular columns, where  $D$  is the diameter of the sections.

$$V_n = V_c + V_s \quad (9)$$

$$V_c = 0.3 \left( k + \frac{P}{14A_g} \right) \sqrt{f_c'} A_e \quad (10)$$

$$0 \leq k = \frac{4 - \mu_\Delta}{3} \leq 1 \quad (11)$$

$$V_s = \frac{\pi A_{sp} f_{yh} d}{2s} \cot 30^\circ \quad (12)$$

### Priestley et al.

Priestley et al. (1996) proposed Eq. (13) through (17) in SI units to calculate nominal shear strength of reinforced concrete columns for design purpose. Considering the effect of displacement ductility,  $V_c$  is calculated by Eq. (14) and (15) for plastic hinge region. The shear strength of reinforcement,  $V_s$ , is calculated by Eq. (16) based on  $35^\circ$  angle truss model for circular columns. The effect of shear strength enhancement, resulting from arch action in axial compression, is considered by Eq. (17). For the columns bent in single curvature, the strut forms between the center of the section at the top where the axial load is applied and the center of flexural compression at the bottom. Therefore  $\tan \alpha$  becomes  $D_c/2L$ , where  $D_c/2$  is the horizontal distance between center of the section and center of flexural compression, and  $L$  is the cantilever column length. In the case of circular sections,  $0.65D$  is recommended for  $D_c$ . The coefficient 0.85 in Eq. (17) is used for seismic design, but 1.0 is suggested for seismic performance evaluation.

$$V_n = V_c + V_s + V_p \quad (13)$$

$$V_c = k \sqrt{f_c'} A_e \quad (14)$$

$$\left( \begin{array}{l} \mu_\Delta \leq 2 : k = 0.25 \\ 2 \leq \mu_\Delta \leq 4 : k = 0.25 - 0.0835(\mu_\Delta - 2) \\ \mu_\Delta = 4 : k = 0.083 \\ 4 \leq \mu_\Delta \leq 8 : k = 0.083 - 0.01025(\mu_\Delta - 4) \\ 8 \leq \mu_\Delta : k = 0.042 \end{array} \right) \quad (15)$$

$$V_s = \frac{\pi A_{sp} f_{yh} D_{sp}}{2s} \cot 35^\circ \quad (16)$$

$$V_p = 0.85P \tan \alpha = 0.85P \frac{D_c}{2L} \quad (17)$$

### Lee et al.

Lee et al. (2006) proposed shear capacity model as shown in Eq. (18) through (22) in SI units, which is basically the same format as Priestley et al.'s model but modified. For the shear strength of concrete,  $k$  in Eq. (19) is modified to Eq. (20) to produce three straight lines divided by the displacement ductility of 2 and 5, while Priestley et al.'s model has four straight lines divided by the displacement ductility of 2, 4, and 8. For the shear strength of reinforcement,  $40^\circ$  angle is adopted as shown in Eq. (21). The axial load effect on shear strength is considered as the same format as Priestley et al.'s model, but  $2/3$  times  $D$  is recommended for  $D_c$  as shown in Eq. (22) for circular sections.

$$V_n = V_c + V_s + V_p \quad (18)$$

$$V_c = k \sqrt{f'_c} A_e \quad (19)$$

$$\left( \begin{array}{l} \mu_\Delta \leq 2 : k = 0.3 \\ 2 \leq \mu_\Delta \leq 5 : k = 0.3 - \frac{1}{10}(\mu_\Delta - 2) \\ 5 \leq \mu_\Delta : k = 0 \end{array} \right) \quad (20)$$

$$V_s = \frac{\pi A_{sp} f_{yh} D_{sp}}{2s} \cot 40^\circ \quad (21)$$

$$V_p = 0.85P \tan \alpha = 0.85P \frac{D_c}{2L} = 0.85P \frac{D}{3L} \quad (22)$$

## Comparison of Models with Test Results

### Selected Experimental Results

In order to compare the ductility based flexure-shear models, two sets of experimental results were selected: (1) four large scale columns tested by the authors, which were previously introduced in this paper, and (2) two large scale column test conducted by Kim et al. (2001).

Kim et al. (2001) conducted quasi-static test for two large scale circular columns, of which diameter was 1200 mm. FS-H-LS000 specimen had 4950 mm of total height and 3200 mm of loading height so that the aspect ratio should be 2.67. The other specimen FS-L-LS000 had 4450 mm of total height and 2700 mm of loading height so that the aspect ratio should be 2.25. The other variables of the two column specimens are identical. Thirty six D25 (diameter of 25.4 mm) reinforcing bars were used for longitudinal steel, which resulted in 0.0161 of longitudinal steel ratio. Circular hoops with 300 mm spacing were used for plastic hinge region so that the volumetric lateral steel ratio should be 0.00169. The space of 300 mm is equivalent to 11.8 times the longitudinal diameter and 23.6 times the transverse steel diameter. The yield stress of D25 and D13 reinforcement were 331 MPa and 326 MPa, respectively. The compressive strength of concrete was measured to be 24.5 MPa at the age of test. More information about the test columns can be found in their paper (Kim et al. 2001).

### Application of Equations for Cross-tie

Three column specimens (MS-HT4 series) tested by the authors have two cross-ties perpendicular to each other. Shear force is resisted by one cross-tie parallel to the lateral loading direction as well as the hoop reinforcement. Shear strength of cross-tie is calculated by Eq. (23), where  $A_{sct}$  is area of cross-tie in a parallel direction to the applied lateral load and  $D_{sp}$  is distance between centers of the perimeter hoop.

$$V_{sct} = \frac{A_{sct} f_{yh} D_{sp}}{s} \cot \theta \quad (23)$$

For MS-HT4 series columns, shear strength of transverse steel,  $V_s$ , is calculated by summation of shear strength produced by hoop reinforcement and cross-tie. When each model is applied, the same value of angle such as  $45^\circ$  (CALTRANS),  $40^\circ$  (Lee et al.),  $35^\circ$  (Priestley et al.) or  $30^\circ$  (Aschheim et al.) is used for  $\theta$  in Eq. (23).

### Failure Mode Prediction

Fig. 7 shows displacement based shear capacity models applied to the envelope curves of test results. The envelope curves are obtained from the measured lateral load-displacement relationship under cyclic loading. Two envelope curves for each column specimen are provided from the test results for push direction and pull direction. The displacement at intersection of the envelope curve and the shear capacity models presents predicted displacement capacity of the column under flexure-shear failure.

For MS-HT4-N-SH specimen which showed flexure-shear failure during the test, CALTRANS model, Aschheim et al.'s model and Lee et al.'s model predict failure mode of flexure-shear failure, but Priestley et al.'s model predicts flexure failure, as shown in Fig. 7(a). For MS-HT4-N-FS specimen which also showed flexure-shear failure during the test, CALTRANS model and Lee et al.'s model predict the same failure mode, but Aschheim et al.'s model and Priestley et al.'s model predict flexure failure, as shown in Fig. 7(b). In the case of MS-HT4-N-L2 specimen, all the models predict the same failure mode as the test result of flexure failure, as shown in Fig. 7(c). For MD-HT6-N-L2, FS-H-S000, and FS-L-S000 specimens which showed flexure-shear failure during the test, all the models predict flexure -shear failure, as shown in Fig. 7(d), (e), and (f). Table 2 presents predicted failure mode by each model. CALTRANS and Lee et al.'s model predict the same failure modes as test result for all the specimens.

Table 2. Failure mode prediction.

Specimens	Failure mode (Test result)	Predicted failure mode by			
		CALTRANS	Aschheim et al.	Priestley et al.	Lee et al.
MS-HT4-N-SH	flexure-shear	flexure-shear	flexure-shear	flexure	flexure-shear
MS-HT4-N-FS	flexure-shear	flexure-shear	flexure	flexure	flexure-shear
MD-HT4-N-L2	flexure	flexure	flexure	flexure	flexure
MD-HT6-N-L2	flexure-shear	flexure-shear	flexure-shear	flexure-shear	flexure-shear
FS-H-LS000	flexure-shear	flexure-shear	flexure-shear	flexure-shear	flexure-shear
FS-L-LS000	flexure-shear	flexure-shear	flexure-shear	flexure-shear	flexure-shear

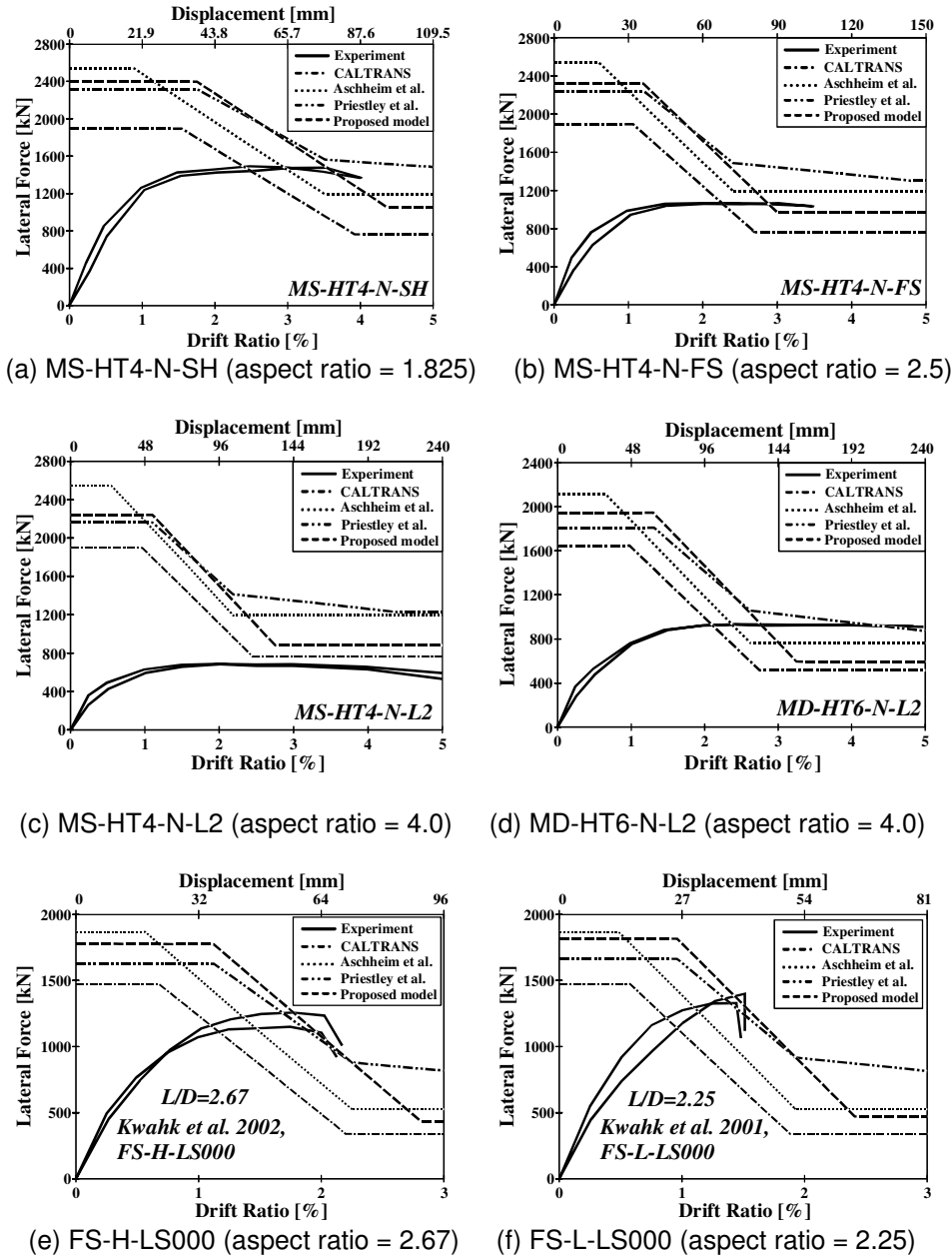


Figure 7. Application of each model for load-displacement of experimental results.

### Accuracy of Displacement Capacity Prediction

Table 3 shows the measured ultimate displacement and the predicted ultimate displacement by the models for 5 specimens under flexure-shear failure. The ratio of predicted ultimate displacement to test result is also presented in Table 3. It is note that Aschheim et al.'s model predicts flexure failure for MS-HT4-N-FS specimen and Priestley et al.'s model predict flexure failure for MS-HT4-N-FS and MS-HT4-N-SH specimen. For five large size columns, the ratio of predicted ultimate displacement by CALTRANS model to test result are between 0.42 and 0.63, while those by Lee et al's model are between 0.54 and 0.98. Aschheim et al.'s model provides the ratio between 0.48 and 0.75 for four column specimens. By Priestley et al.'s model, three specimens show the ratio between 0.86 and 0.93.



Table 3. Predicted ultimate displacement and accuracy.

Specimens	Ultimate displacement (mm)					Ratio of predicted ultimate displacement to test result			
	Test	CAL-TRANS	Aschheim et al.	Priestley et al.	Lee et al.	CAL-TRANS	Aschheim et al.	Priestley et al.	Lee et al.
MS-HT4-N-SH	88	54	66	-	79	0.61	0.75	-	0.90
MS-HT4-N-FS	105	66	-	-	86	0.63	-	-	0.82
MD-HT6-N-L2	240	101	115	206	130	0.42	0.48	0.86	0.54
FS-H-LS000	69	36	46	57	60	0.52	0.67	0.83	0.87
FS-L-LS000	40	25	30	37	39	0.63	0.75	0.93	0.98

### Conclusions

Four large size columns were tested to investigate the shear related behavior under cyclic lateral load. In addition to those columns, two more large size columns, tested by other researchers, were selected and the displacement based flexure-shear capacity models were applied to the test columns. The predicted displacement capacity by each model was compared with test result and the accuracy was investigated. It may not be fully adequate to derive a final conclusion from the limited number of test results; however the CALTRANS model and Lee et al.'s (2006) model provide better predictions for failure mode than the other models. For ultimate displacement prediction, Lee et al.'s (2006) model provides closer results to the test than the other models.

### Acknowledgments

Support for this work was provided by the Korea Bridge Design & Engineering Research Center (KBRC). This financial support is gratefully acknowledged.

### References

- AASHTO, 2002. *LRFD Bridge Design Specifications*, American Association of State Highway and Transportation Officials, 2nd ed., Washington, D.C., USA.
- Aschheim, M. and Moehle, J. P., 1992. Shear Strength and Deformability of RC Bridge Columns Subjected to Inelastic Cyclic Displacement, *Report No. UCB/EERC 92/04*, Earthquake Engineering Research Center, University of California at Berkeley.
- CALTRANS, 2006. *Caltrans Seismic Design Criteria*, Version 1.4, California Department of Transportation, Sacramento, USA.
- Chung, Y.S., Lee, J.H., and Kim, J.K., 2001. Experimental Research for Seismic Performance of Existing Reinforced Concrete Piers, *Research Report*, Korean Highway Corporation, Seoul, Korea.
- Kim, B.S., Kim, Y.J., Kwahk, I.J., Cho, C.B., and Cho, J.R., 2001. Seismic Performance Evaluation of Circular RC Bridge Piers with Shear Flexure Behavior, *Journal of the Earthquake Engineering Society of Korea*, 5 (3). 29-36.
- Korean Ministry of Construction and Transportation, 2005. *Korean Bridge Design Specifications*, Seoul, Korea.
- Lee, J.H., Ko, S.H., and Chung, Y.S., 2006. Shear Capacity Curve Model for Circular RC Bridge Columns under Seismic loads, *Journal of the Earthquake Engineering Society of Korea*, 10 (2), 1-10.

Priestley, M. J. N., Seible, F., and Calvi, G. M., 1996, *Seismic Design and Retrofit of Bridges*, John Wiley & Sons, Inc., New York.